Ten Years of N-Heteropentacenes as Semiconductors for Organic Thin-Film Transistors

*Qian Miao**

Introducing N atoms to the pentacene backbone leads to N-heteropentacenes, whose properties can be tuned by changing the number, position and valence state of N atoms in the pentacene backbone. With a rapid development in recent years, N-heteropentacenes and their derivatives have arisen as a new family of organic semiconductors with high performance in organic thin-film transistors (OTFTs). This article reviews the research efforts of developing N-heteropentacenes into organic semiconductors starting from 2003 with emphasis on the work of the author's group since 2009. The structure–property relationship and design rationale are highlighted based on an overview of reported organic semiconductors of N-heteropentacenes.

1. Introduction

Polycyclic aromatic hydrocarbons (PAHs) are an important class of organic semiconductors. By analogy with silicon-based inorganic semiconductors that are commonly doped by atomic substitution in silicon solids with group III and V elements, can PAH-based organic semiconductors be engineered by replacing carbon atoms with group III and V elements, such as B and N atoms? Driven by such curiosity, B and N atoms have been introduced to the π-backbones of PAHs resulting in interesting heteroarene molecules that are structurally similar to their hydrocarbon analogues but show different properties.[1,2] A particularly interesting subgroup of these heteroarenes is the N-heteropentacenes, which formally result from inserting N atoms into pentacene, a leading p-type organic semiconductor for applications in organic thin-film transistors (OTFTs). Such interest mainly arose from the promise of tuning the electronic structure, molecular packing, stability, and processability of pentacene by replacing C atoms with N atoms of varied number, position, and valence state. Although the history of N-heteropentacenes and other N-heteroacenes can be traced back more than a century,[3,4] this family of π-conjungated molecules were underdeveloped until 2003, when they were demonstrated to function as organic semiconductors in OTFTs.[5] This article, after a very brief introduction to OTFTs, reviews the research efforts of developing N-heteropentacenes into organic semiconductors in the past 10 years with emphasis on the work of the author's group. To complement a few recently published reviews on N-heteropentacenes and other N-heteroacenes,[6,7] this article highlights structure–property relationships and design rationale based on an overview of reported organic semiconductors of N-heteropentacenes, including the most recent examples.

OTFTs are elemental units in organic integrated circuits that, for example, operate radio-frequency identification (RFID) tags and sensors and are used to drive individual pixels in active matrix displays.[8,9] For these applications, OTFTs can be fabricated onto flexible substrates over a large area at low cost using roll-to-roll or inkjet printing techniques. Low-power complementary circuits utilize both positive and negative gate voltages to switch transistors and thus require both p- and n-channel transistors. N-channel OTFTs are based on n-type semiconductors to conduct electrons and achieve their high-conductivity "on" state with positive gate voltages, whereas the majority of OTFTs reported to date are p-channel transistors, which conduct holes with p-type semiconductors and are turned on with negative gate voltages. The most important parameter to characterize the performance of OTFTs is field-effect mobility (μ_{FET}), which quantifies the average charge-carrier (hole or electron) drift velocity per unit of electric field. With field-effect mobility reaching or exceeding that of amorphous silicon (about 1 $cm^2\ V^{-1}\ s^{-1}$), leading organic semiconductors can be used for applications that require sharp turn-on and fast switching. The ultimate success of OTFTs requires organic semiconductors that have high field-effect mobility, robust environmental stability, and easy processability. N-type organic semiconductors that can meet all the requirements are still a challenge for the research of organic semiconductors, primarily due to the inherent instability of organic anions in the presence of air and water and problems with oxygen trapping within these materials.[10]

Two key factors of organic semiconductors that determine their performance in OTFTs are electronic structure and molecular packing in the solid state. As concluded by Bao and coworkers on the basis of a series of functionalized acene derivatives, a quantitative relationship between molecular orbital energy levels and the charge carrier type in OTFTs is that the highest occupied molecular orbital (HOMO) energy level of a semiconductor molecule should be –5.60 eV or higher to allow

Prof. Q. Miao
Department of Chemistry
the Chinese University of Hong Kong
Shatin, New Territories, Hong Kong, PR China
Institute of Molecular Functional Materials
(Areas of Excellence Scheme
University Grants Committee)
Hong Kong, China
E-mail: miaoqian@cuhk.edu.hk

DOI: 10.1002/adma.201305497

p-channel field effect, and the lowest unoccupied molecular orbital (LUMO) energy level of a semiconductor molecule should be −3.15 eV or lower to allow n-channel field effect.[11] The charge-transport properties of organic semicodnuctors at the microscopic level are governed by electronic coupling between neighboring molecules, in a way that intimately depends on both the relative positions of interacting molecules and the phase and nodal properties of frontier molecular orbitals. As concluded by Brédas and coworkers from their theoretical investigations,[12] the charge-carrier mobility is determined by the amplitude of the electronic transfer integrals between adjacent semiconductor molecules rather than the "spatial overlap" between π-orbitals. One attractive aspect of N-heteropentacenes as organic semiconductors is that their electronic structure and molecular packing can both be tuned by changing the number, position, and valence state of N atoms in the pentacene backbone. One key question that has driven research into N-heteropentacenes is how many C atoms in pentacene need to be replaced by N atoms in order to convert pentacene into an n-type semiconductor. Moreover, because OTFTs are interface devices, with their performance being highly dependent on the interface between organic semiconductors and gate dielectrics, interface structures and properties are as important to OTFTs as organic semiconductor materials. Therefore this review also discusses interface engineering strategies for vacuum-deposited and solution-processed OTFTs of N-heteropentacenes.

2. Non-Substituted N-Heteropentacenes: The First-Generation Semiconductors

Most of the known N-heteropentacenes contain pyrazine and/or its reduced form, dihydropyrazine, in their polycyclic backbones since they can be conveniently synthesized by conventional condensation reactions or by recently developed palladium-catalyzed N-arylation reactions.[13] These molecules are also referred to as pyrazinacenes and have a history of more than 120 years. As shown in **Figure 1**a, the first documented N-heteropentacenes were 5,14-dihydro-5,7,12,14-tetraazapentacene (**1**) and 6,13-dihydro-6,13-diazapentacene (**2**), which were synthesized by Fischer and Hepp in 1890[3] and by Hinsberg in 1901,[4] respectively. After the first synthesis, N-heteropentacenes were underdeveloped for a century. The methanesulfonate salt of **1** was reported to behave as a semiconductor with a conductivity of about 10^{-2} S cm^{-1} at room temperature,[14] and an ultraviolet photoelectron spectroscopy (UPS) study suggested **1** could be used as an electron-transporting material in organic light-emitting diodes.[15] However, these studies received little attention. A milestone was made in 2003, when Nuckolls, Miao and coworkers demonstrated that **2** and its constitutional isomer **3** (shown in Figure 1a) functioned as p-type organic semiconductors in OTFTs with field-effect mobilities of 5×10^{-5} and 6×10^{-3} cm^2 V^{-1} s^{-1}, respectively.[5] Two years later, **1** was also reported to be a p-type semiconductor exhibiting field-effect mobility of up to 0.02 cm^2 V^{-1} s^{-1} in OTFTs.[16]

Despite the pioneering work on OTFTs of **1–3**, it remained a question as to whether a N-heteropentacene molecule was able to achieve high field-effect mobility comparable to that of pentacene until **2** was reinvestigated by the author's group in 2009.[17] This study showed that the field-effect mobility of **2** could be dramatically enhanced by tuning the structure of the dielectric surface. The vacuum-deposited films of **2** exhibited three crystalline polymorphs depending on the surface structure and the temperature of the substrate. When **2** was deposited on octadecyltrichlorosilane (OTS)-treated SiO_2 at a substrate temperature of 100 °C, the resulting "12.9 Å-phase" films yielded mobilities as high as 0.45 cm^2 V^{-1} s^{-1}, which is over 5000 times higher than those of the other two phases and is comparable to that of pentacene in control experiments. This unusually large effect of crystalline polymorphs on charge transport was attributed to subtle changes of molecular packing in different polymorphs in relation to the relative positions of interacting molecules and the phase and nodal properties of HOMO. The reinvestigation of **2** led to two conclusions: first, N-heteropentacenes are of great potentials for high-mobility OTFTs; and, second, interface engineering is of key importance to high-performance N-heteropentacene OTFTs.

Following **1–3**, non-substituted N-heteropentacenes **4–6** (shown in Figure 1a) were applied as organic semiconductors in OTFTs. It was found that **4** and **5** functioned as p-type semiconductors with field-effect mobilities of up to 7×10^{-4} and 8×10^{-5} cm^2 V^{-1} s^{-1}, respectively,[18,19] while **6**, with a LUMO energy level as low as −4.00 eV, functioned as an n-type semiconductor exhibiting field-effect mobility of 4×10^{-4} cm^2 V^{-1} s^{-1}.[20] The low mobility of **4** can be attributed to the amorphous nature of its vacuum-deposited films, and the low mobility of **6** is likely related to its unstable thin film, which quickly changes into isolated crystal domains. Because the reduced form **2** is isostructural to pentacene while the oxidized form **5** is isoelectronic to pentacene, **2** and **5** are interesting subjects for studying structure–property relationships. Since a complete comparison has already been made in an earlier review,[7] discussed here are mainly the electronic structure as well as molecular packing.

Prof. Qian Miao was born in 1977 in Chengdu, China, and graduated from the University of Science and Technology of China with a B.Sc. degree in 2000. He received his Ph.D. degree from Columbia University in 2005 under the direction of Prof. Colin Nuckolls, and did postdoctoral research with Prof. Fred Wudl at the University of California, Los Angeles for one year. He joined the Chinese University of Hong Kong as an assistant professor in 2006 and was promoted to Associate Professor in 2012. His research is directed at functional organic materials with high performance and novel function, and currently focuses on organic semiconductor materials and devices as well as novel non-planar π-molecules.

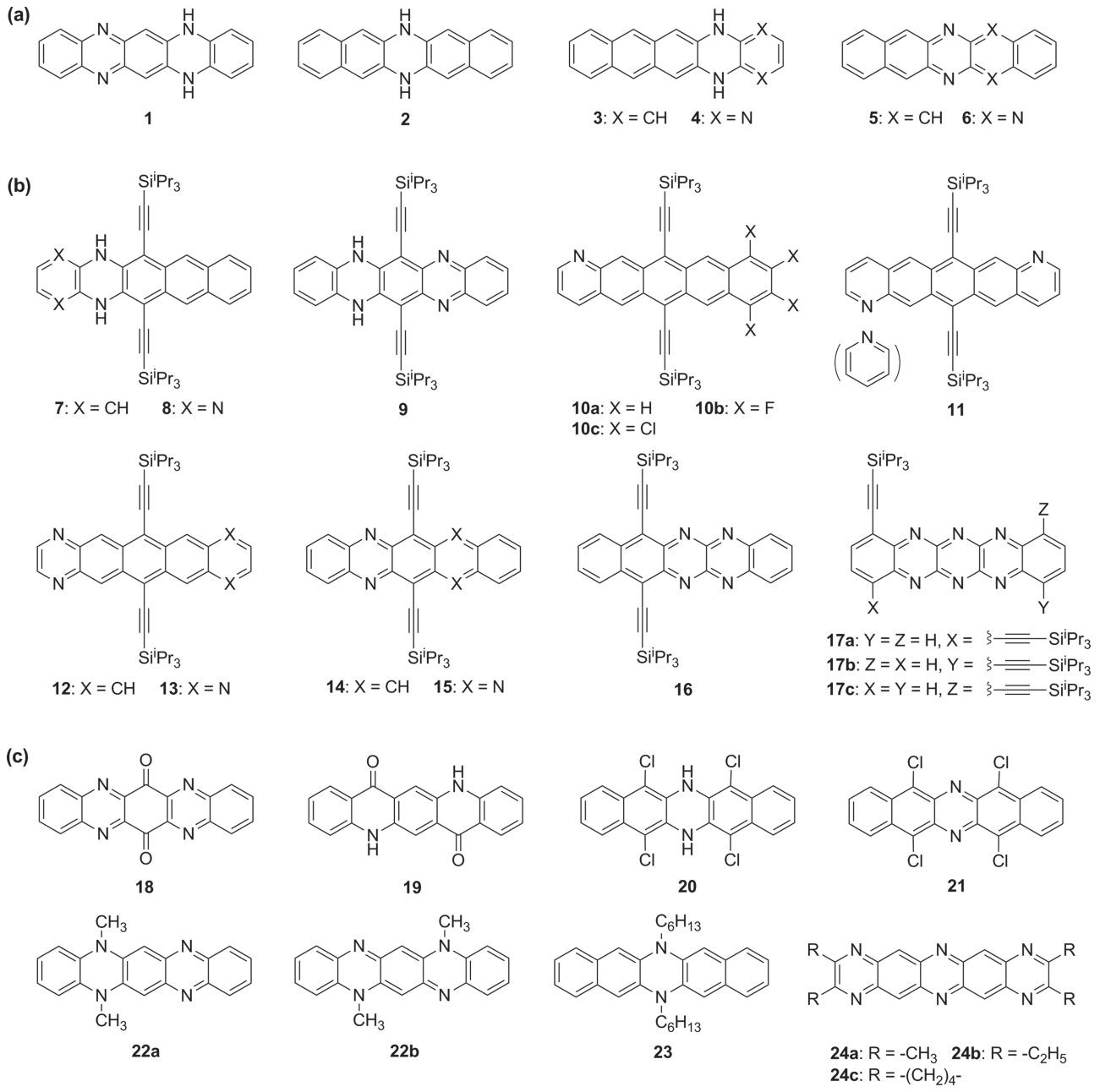

Figure 1. Molecular structures of N-heteropentacenes and their derivatives: a) non-substituted N-heteropentacenes that were demonstrated as organic semiconductors in OTFTs; b) silylethynylated N-heteropentacenes; and, c) other N-heteropentacene derivatives.

The HOMO energy levels of **2** and **5** are –4.63 and –5.56 eV, respectively; and the LUMO energy levels of **2** and **5** are –1.80 and –3.63 eV, respectively. The low field-effect mobility of **5** may be attributed to its unstable cation, as suggested by the relatively low HOMO energy level and the absence of oxidation waves in the cyclic voltammogram. The less stable the cation of organic semiconductor, the more easily the cation is quenched by defects in thin films, leading to poor charge transport. Another issue related to electronic structure is stability, which is of practical importance to organic semiconductors. Although **2** has 24 π-electron and a formally anti-aromatic dihydropyrazine ring, it is a stable compound resisting oxidation when its solution is exposed to air and ambient light at room temperature for at least one day. **2** is thermodynamically stabilized by two factors: first, the dihydropyrazine is stabilized by four enamine conjugations, as revealed by Bunz's computational study;[21] and, second, breaking a pentacene into two naphalenes is advantageous according to Clar's sextet rule. Moreover, **2** is kinetically stable toward self-sensitized photooxidation that degrades pentacene likely because **2** only weakly absorbs visible light and its HOMO mismatches with the LUMO of singlet oxygen in terms of symmetry.

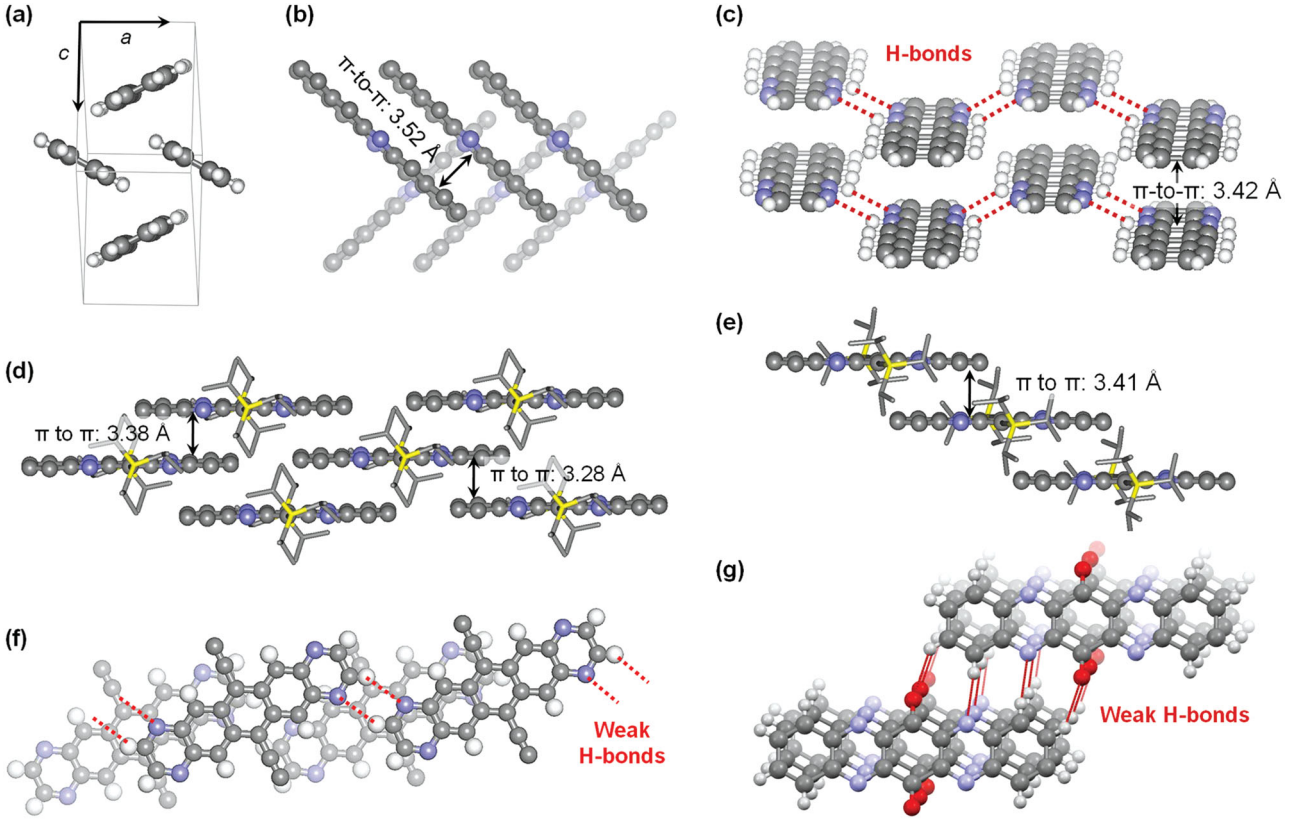

Figure 2. Representative molecular packing modes of N-heteropentacenes and derivatives: a) herringbone packing of **2**, b) offset π-stacking of **5**, c) H-bonded ribbons of **4** with π-stacking, d) two-dimensional π-stacking of **15** with brickwork arrangement, e) one-dimensional π-stacking of **9**, f) bilayer π-stacks of **13** with C–H···N hydrogen bonds, g) quadruple weak H-bonds and offset π-stacking of **18**. For clarity, the N-heteropentacene cores are shown with ball–stick models and the silylethynyl substituents are shown with stick models, hydrogen atoms are removed in (d) and (e), and triisopropylsilyl groups are removed in (f). (a) and (d) reproduced with permission.[7] Copyright 2012, Thieme. (c) is reproduced with permission.[19] Copyright 2012, American Chemical Society. (d)-(f) are reproduced with permission.[30] Copyright 2011, Wiley-VCH.

Non-substituted N-heteropentacenes **2** and **4–6** exhibit different packing modes in crystals in relation to the property and pattern of N atoms. **2** exhibits a herringbone packing that is also characteristic of pentacene, as shown in **Figure 2**a. The common herringbone packing of **2** and pentacene is in agreement with their electron-rich π-planes and almost identical σ-framework according to Hunter and Sanders' model.[22] In connection to the π-electron-deficient nature, **5** and **6** exhibit offset π-stacking with lateral shifts. Shown in Figure 2b is the molecular packing of **5** with a distance of 3.52 Å between neighboring π-planes.[7] Unlike **2**, **5**, and **6**, dihydrotetraazapentacene **4** is capable of H-bonds. As shown in Figure 2c, molecules of **4** form H-bonded ribbons that stack in two directions. In each ribbon, molecules of **4** are linked by double N–H···N H-bonds with a N-to-N distance of 3.05 Å. Two π-stacked molecules of **4** are separated by a distance of 3.42 Å between π-planes and have an offset arrangement along the long molecular axis.

The above non-substituted N-heteropentacenes (**1–6**) can be considered as first-generation organic semiconductors based on N-heteropentacenes, which are all vacuum-deposited p-type semiconductors. Although some of them are soluble in dimethylformamide (DMF) and dimethyl sulfoxide (DMSO) with solubility higher than 1 mg mL^{-1}, these solvents are not suitable for solution processing because it is very difficult to remove hydrogen-bonded solvent molecules from the crystal lattice of N-heteropentacenes without destroying the films. To achieve n-type semiconductors with N-heteropentacenes, on the basis of density function theory (DFT) calculation, Winkler and Houk concluded that at least seven N atoms have to be incorporated into pentacene.[23] Chen and Chao also identified a decaazapentacene as a potentially suitable n-type semiconductor for OTFTs.[24] However, the proposed non-substituted heptaazapentacenes and decaazapentacene are still challenging targets for synthesis, and likely too unstable to be prepared. Therefore, solution-processed n-type semiconductors based on N-heteropentacenes requires suitable substituting groups to lower the LUMO energy level and to enhance solubility as well as stability.

3. Silylethynylated N-Heteropentacenes: The Second-Generation Semiconductors

Following the great success of 6,13-bis(triisopropylsilylethynyl) pentacene (TIPS-PEN) and other silylethynylated pentacenes as stable and solution-processable organic semiconductors

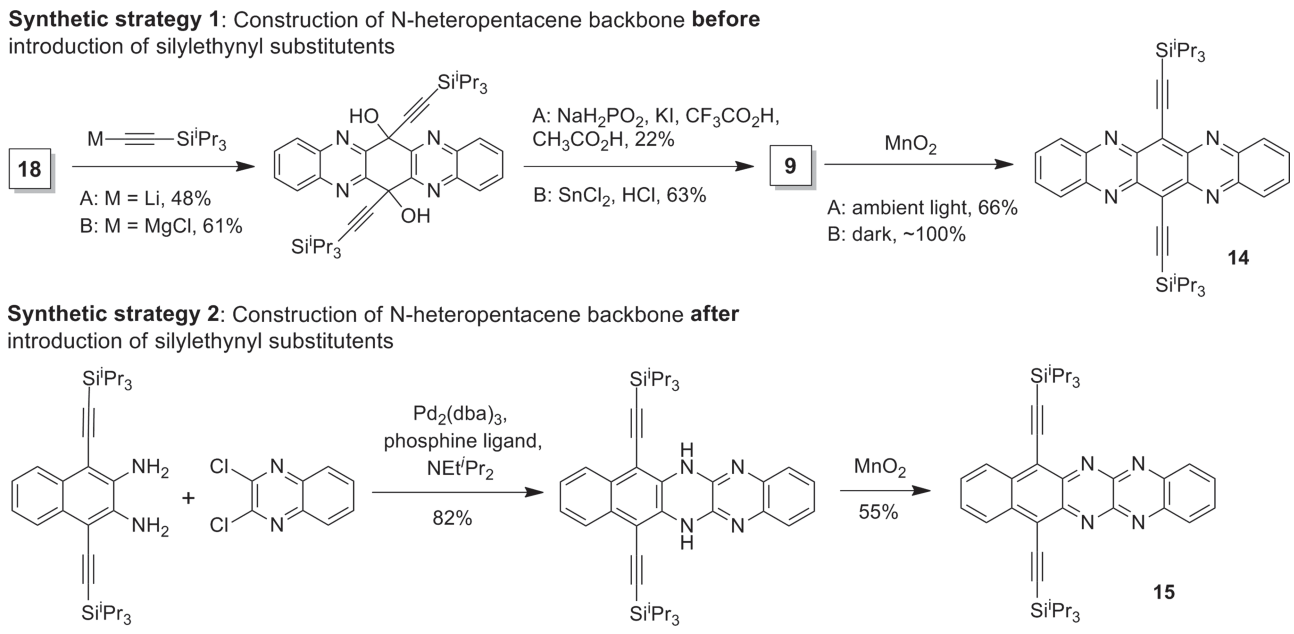

Scheme 1. Representative synthesis of silylethynylated N-heteropentacenes.

with high charge-carrier mobilities,[25] introducing silylethynyl groups to N-heteropentacenes became a promising strategy to develop second-generation organic semiconductors based on N-heteropentacenes. The use of silylethynyl groups has several advantages. First, the roughly spherical trialkylsilyl groups attached to the linear alkyne moieties allow exquisite control over the solid-state arrangement,[25] and the triisopropylsilyl group is particularly powerful to induce two-dimensional π-stacking with brickwork arrangement. Second, ethynyl groups lower the LUMO energy level by withdrawing electrons because *sp* carbons are more electronegative than sp^2 carbons. Third, the trialkylsilyl groups dramatically increase solubility. Fourth, alkynyl functionalization at the 6 and 13 positions of pentacene reduces the rate of photooxidation by lowering the LUMO energy level and by reducing the triplet energy, thereby preventing singlet oxygen sensitization.[26]

The first step to investigate silylethynylated N-heteropentacenes is synthesis. As one of the pioneers in this field, Bunz first synthesized a series of silylethynylated N-heteropentacenes by modifying the known syntheses of TIPS-PEN and non-substituted N-heteroacenes.[27] Later on, Bunz and coworkers developed palladium-catalyzed N-arylation reactions to synthesize silylethynylated N-heteroacenes that were synthesized with difficulty or inaccessible previously.[13,28] As shown in **Scheme 1**, the synthesis of silylethynylated N-heteropentacenes can be roughly classified into two routes depending on the sequence of reactions. The first route has silylethynyl groups attached to a pre-formed N-heteropentacene backbone by nucleophilic addition or Sonogashira coupling, while the second constructs the N-heteropentacene backbone, typically by palladium-catalyzed N-arylation, from a silylethynyl-substituted acenediamine.

Using the two general synthetic strategies with modifications, a variety of silylethynylated N-heteropentacenes were synthesized. As shown in Figure 2b, Zhang reported a series pyridine-containing N-heteropentacenes (**10a–c** and **11**),[29] and the author's group systematically studied a series of pyrazine-containing N-heteropentacenes with varied number and position of N atoms (**7–9**, **12–15**, and **17a–c**).[19,30,31] Along with tetraazapentacene **16** synthesized by Bunz, these molecules provide a good opportunity to study structure–property relationships, particularly, to answer the question as to how many N atoms are sufficient and where these N atoms should be introduced in order to achieve n-type organic semiconductors. Summarized in **Table 1** are HOMO and LUMO energy levels of **7–17**. For comparison, silylethynylated N-heteropentacenes with extra halogen substituents are excluded from this table. The reduced-form N-heteropentacenes **7–9** have 24 π-electrons. In agreement with this, **7–9** have experimental HOMO energy levels higher than −5.20 eV and experimental LUMO energy level higher than −3.00 eV. In contrast, **10–17** are the oxidized form with 22 π-electrons. As expected, from **10a** to **17a**, the LUMO energy level is lowered with the increased number of N atoms. A somewhat unpredictable finding from Table 1 is that replacing an internal benzene ring of pentacene backbone with a pyrazine ring is more effective in lowering HOMO and LUMO energy levels than replacing a terminal benzene ring. With three internal pyrazine rings, **17a** reaches a LUMO energy level lower than −4.50 eV, and is gradually reduced with an obscure mechanism when its solutions or solids are stored in air under ambient light for several days.[31] The LUMO energy levels of **10–16** and the instability of **17a–c** suggest that to be stable n-type semiconductors, silylethynylated N-heteropentacenes would better have at most six unsaturated nitrogen atoms.

Most of the known silylethynylated N-heteropentacenes have two triisopropylsilyl (TIPS) substituents, which are a dominating factor to control the molecular packing. Except

Table 1. HOMO and LUMO energy levels and field-effect mobility of silylethynylated N-heteropentacenes.

Compound	HOMO [eV]		LUMO [eV]		Field-effect mobility [$cm^2 V^{-1} s^{-1}$][a)]			
					Hole		Electron	
	Exp.	Calcd.	Exp.	Calcd.	Exp.	Calcd.	Exp.	Calcd.
7[30a,7]	−5.06	−5.05	−2.66	−2.08	0.02–0.07	0.71[33]	No field effect	0.03[33]
						3.12[32]		0.11[32]
8[19]	−5.17	−5.41	−2.66	−2.33	0.3–0.7	0.01[31]	No field effect	0.07[33]
9[30a,7]	−5.14	−5.30	−2.97	−2.52	No field effect	0.06[33]	No field effect	0.02[33]
						0.22[32]		0.045[32]
10a[29a]	−5.31	−4.95	−3.33	−3.13	0.22	Not reported	No field effect	Not reported
11[30]	−5.42	−5.09	−3.40	−3.24	0.11	0.58[32]	0.15	7.44[32]
12[30b]	−5.25	−5.19	−3.49	−3.35	0.3–1.2	0.21[33]	No field effect	5.01[33]
						0.34[32]		7.15[32]
13[30b]	−5.49	−5.44	−3.68	−3.59	0.05–0.22	Not reported	0.3–1.1	Not reported
14[30a,7]	−5.34	−5.28	−3.68	−3.48	0.02–0.05	0.005[33]	$2–4\times10^{-4}$	1.24[33]
						0.12[32]		5.57[32]
15[30a,7]	−5.75	−5.64	−4.01	−3.81	No field effect	0.02[33]	1.0–3.3 [b)]	0.25[33]
						0.0067[32]	1.0–2.5 [c)]	4.99[32]
16[13]	Not reported	−5.48	−4.28	−3.59	Not reported	Not reported	Not reported	Not reported
17a[31]	−6.14	−6.24	−4.54	−4.32	Not reported	Not reported	Not reported	Not reported

[a)]The hole mobility was measured in ambient air and the electron mobility was measured under vacuum; [b)]Measured from vacuum-deposited OTFTs;[30a]; [c)]Measured from solution-processed OTFTs.[34]

for **10a**, **10c**, and **17a–c**, all the molecules shown in Figure 1b have their crystal structures established by X-ray crystallography. Most of these silylethynylated N-heteropentacenes share the same type of molecular packing, namely two-dimensional π-stacking with brickwork arrangement, although they have different π-backbones with N atoms of varied number, position, and valence state and even different substituting positions for ethynyl groups. As an example of this type of π-stacking, the molecular packing of **15** is shown in Figure 2. Molecules **9** and **13** differentiate themselves from most of the silylethynylated N-heteropentacenes by packing in different modes. Molecules of **9** are arranged in one-dimensional π-stacks as shown in Figure 2e. On the basis of DFT calculations, such arrangement was attributed to strong C–H$\cdots\pi$ interactions between the TIPS group and the pyrazine ring in relation to the negatively charged N atoms in the pyrazine ring of **9**.[32] Molecules of **13** exhibit an even more different packing mode featuring bilayer π-stacks with C–H$\cdots$N hydrogen bonds. As shown in Figure 2f molecules of **13** are first linked by double C–H$\cdots$N hydrogen bonds to form a ribbon-like structure, and two H-bonded ribbons of **13** then form bilayer π-stacks, which are arranged in a herringbone motif. The unique molecular packing of **13** can be attributed to the exposed N atoms, which allow C–H$\cdots$N hydrogen bonds to play an important role in controlling molecular packing. On the other hand, **12** keeps the π-stacking of brickwork arrangement likely because one pyrazine ring is still not enough to change the molecular packing with hydrogen bonds. It is worth noting that among the silylethylated N-heteropentacenes without extra substituents, **16** has the closest packing with a volume per molecule of 929.404 $Å^3$, and the second is **15**, which has a volume per molecule of 944.346 $Å^3$. In contrast, **9** has the loosest packing, occupying a volume of 1015.99 $Å^3$ per molecule.

All the silylethynylated N-heteropentacenes shown in Figure 1b, except **9**, **16**, and **17a–c**, were reported to function as semiconductors in OTFTs. With the reported molecular packing in crystals, the charge-transport properties of these silylethynylated N-heteropentacenes were also calculated by Shuai[32] and Ren.[33] The measured and calculated field-effect mobilities are summarized in Table 1. Most of these mobilities are measured from vacuum-deposited OTFTs, although the silylethynylated N-heteropentacenes are soluble in a wide range of organic solvents. The solution-processed OTFTs of **15** was not reported until very recently.[34] The reduced-form N-heteropentacenes **7** and **8** were reported to function as only p-type semiconductors, in agreement with their high HOMO and LUMO energy levels. The field-effect mobility of **8** was measured as up to 0.7 $cm^2 V^{-1} s^{-1}$, but its constitutional isomer **9** appeared insulating in polycrystalline films without any field effect. Pyridine-containing heteropentacenes **10a** and **11** behaved as p-type and ambipolar semiconductors, respectively, although the LUMO energy level of **11** is only slightly lower than that of **10a** by 0.07 eV.[29a] With extra electron-withdrawing halogen substitutents, **10b** and **10c** had LUMO energy levels lower than that of **10a** by 0.13 and 0.20 eV, respectively; in agreement with this, they both behaved as ambipolar semiconductors in OTFTs. In particular, **10c** exhibited balanced hole and electron mobilities of 0.12 and 0.14 $cm^2 V^{-1} s^{-1}$, respectively.[29b] Among the pyrazine-containing heteropentacenes, **12** behaved as a p-type semiconductor and **15** behaved as an n-type semiconductor,

while **13** and **14** behaved as ambipolar semiconductors showing field effect in both p- and n-channel OTFTs, in agreement with the HOMO and LUMO energy levels. Both **13** and **15** exhibited electron mobility exceeding 1.0 $cm^2\ V^{-1}\ s^{-1}$ as measured under vacuum. When the OTFTs were tested in ambient air, the measured electron mobility of **13** and **15** decreased to 10^{-3} and 0.5 $cm^2\ V^{-1}\ s^{-1}$, respectively. The poorer environmental stability of **13** is related to its higher LUMO energy level because injection of electrons into such a higher LUMO leads to less stable anions, which are more easily quenched by oxygen and water. Tetraazapentacene **16**, the constitutional isomer of **13** and **15**, is a promising candidate for n-type semiconductors with a LUMO energy level of –4.28 eV and two-dimensional π-stacking, but has not been tested in OTFTs to date.[13] On the other hand, attempts to fabricate OTFTs of **17a–c** appeared to be unsuccessful because these compounds decomposed during thermal evaporation and formed disordered films with poor morphology during solution-based processing.[31]

The best semiconductor from silylethynylated N-heteropentacenes is **15**, which exhibited electron mobility in the range 1.0–3.3 $cm^2\ V^{-1}\ s^{-1}$ as measured from vacuum-deposited OTFTs under vacuum. High-performance solution-processed OTFTs of **15** were recently achieved by drop-casting a solution of **15** on a self-assembled monolayer of newly developed phosphonic acid with enhanced surface energy.[34] With this interface engineering strategy, the solution-processed OTFTs of **15** achieved field-effect mobility as high as 2.5 $cm^2\ V^{-1}\ s^{-1}$. The average field-effect mobility of these solution-processed OTFTs was 1.6 $cm^2\ V^{-1}\ s^{-1}$, the same as the average mobility measured from the vacuum-deposited OTFTs. This allows **15** to be one of the best-performing n-type organic semiconductors. Besides interface engineering, another factor that determines the performance of **15** in OTFTs is the quality of materials, which greatly depends on the details of synthesis. Unlike that prepared by a modified synthesis (Condition B as shown in Scheme 1), the material of **15** as prepared exactly following Bunz's first synthesis (Condition A as shown in Scheme 1) exhibited much lower field-effect mobility (about 0.1 $cm^2\ V^{-1}\ s^{-1}$) likely because of its lower purity.

Finding the relationship between the measured field-effect mobilities and the fine structures of silylethynylated N-heteropentacenes is of great importance to designing new semiconductors based on N-heteropentacenes. However, quantitative explanation of the measured mobilities remains a challenge. As shown in Table 1, there is a considerable gap between the measured and calculated mobilities for most of the silylethynylated N-heteropentacenes. This discrepancy can be, at least partially, explained in terms of the imperfect nature of polycrystalline thin films, such as impurities and grain boundaries. It is worth noting that the calculated mobility is based on an assumption of effective charge injection from the electrode to organic semiconductors. However, effective charge injection may not be realized experimentally for the molecules with high LUMOs, which leads to a significant energy barrier for charge injection from metal electrodes, typically gold. Moreover, mobile electrons flow in the active channel of OTFTs by hopping from the LUMO of one semiconductor molecule to another. Therefore, a higher LUMO energy level in an organic semiconductor is associated with higher-energy mobile electrons, which have a greater chance to be trapped by defects in the thin films even if oxygen and water are excluded by conducting electrical measurement under vacuum or inert atmosphere. Therefore the relatively high LUMO energy level can be a reason for not only the absence of n-channel field effect from the films of **7–9**, **10a**, and **12**, but also the measured electron mobility of **14**, which is four orders of magnitude lower than the calculated values. On the other hand, although calculations predicted that **9** is a better p-type semiconductor than **8** for OTFTs, **9** did not show any field effect in the experiments. As **9** and **8** both formed highly ordered films with similar film morphology, the large discrepancy between experimental and computational results questions the validity of the computation method.

4. Other N-Heteropentacene Derivatives

N-heteropentacenes can be derivatized by attachment of substituents to C or N atoms. Oxidation of **1** with dichromate in sulfuric acid yielded tetraazapentacenequinone **18** (shown in Figure 1c). Equipped with electron-withdrawing quinone and pyrazine moieties, **18** has a LUMO energy level of –3.78 eV. Molecules of **18** form offset π-stacks in two directions with a π–π distance of 3.37 Å and quadruple weak C–H···N/O H-bonds of a self-complementary DDAA-AADD pattern between neighboring π-stacks (shown in Figure 2g). It was found that **18** behaved as an n-type semiconductor in vacuum-deposited OTFTs with field-effect mobility of 0.04 to 0.12 $cm^2\ V^{-1}\ s^{-1}$ as measured under vacuum. Quinacridone (**19** as shown in Figure 1c), a widely used magenta pigment, is structurally related to **18** by having two carbonyl groups embedded in a N-heteropentacene. Unlike the unsaturated N atoms in **18**, the N atoms in **19** are saturated and electron-donating. In agreement with this, **19** has HOMO and LUMO energy levels of –5.5 and –2.9 eV, respectively. Głowacki and coworkers fabricated OTFTs of **19** by vacuum-depositing **19** onto an Al_2O_3 dielectric that was passivated by a layer of tetratetracontane ($C_{44}H_{90}$) and using gold as top-contact electrodes. It was found that **19** behaved as an ambipolar semiconductor with a hole mobility of 0.2 $cm^2\ V^{-1}\ s^{-1}$ as measured in air and an electron mobility of 0.01 $cm^2\ V^{-1}\ s^{-1}$ as measured under a nitrogen atmosphere.[35] The n-channel field effect of **19** is unusual in view of the fact that the LUMO energy level of **19** is higher than –3.0 eV.

Direct chlorination of **2** by SO_2Cl_2 led to chlorinated derivative **20**, which was oxidized with copper (II) acetate and air yielding **21** (shown in Figure 1c). Both **20** and **21** were tested by Tao and coworkers in OTFTs as well as single-crystal organic field-effect transistors (OFETs).[36,37] With a LUMO energy level as low as –3.79 eV, **21** functioned as an n-type semiconductor in the transistors fabricated directly on single crystals and exhibited very high electron mobility in the range of 2.50 to 3.39 $cm^2\ V^{-1}\ s^{-1}$ as measured under ambient conditions. In comparison, **20** did not show any field effect in its films deposited on SiO_2/Si, but functioned as a p-type semiconductor when deposited on a pentacene buffer layer exhibiting a hole mobility as high as 1.4 $cm^2\ V^{-1}\ s^{-1}$. However, this high mobility is not only from **20**, and the contribution from pentacene in the active channel should not be ignored.

Deprotonation of **1** with butyl lithium followed by treatment with methyl iodide yielded benzenoid and quinonoid isomers, **22a** and **22b** (shown in Figure 1c), respectively.[38] Both the two molecules exhibit offset π-stacking in the crystals, although the backbone of **22a** bends at the methylated N atoms with a bending angle of 160°, while **22b** is planar. With a HOMO energy level of –5.01 eV for **22a** and –4.79 eV for **22b**, they both functioned as p-type semiconductors in OFETs fabricated on thin crystals showing low field-effect mobilities in the range of 10^{-4} cm^2 V^{-1} s^{-1}. A similar alkylation reaction of **2** yielded **23**, which has a HOMO energy level of –4.76 eV.[39] As found from the single crystal structure, **23** has a planar π-backbone and exhibits offset π-stacking with a π-to-π distance of about 3.5 Å. In vacuum-deposited OTFTs, **23** behaved as a p-type semiconductor with a field-effect mobility of 3.2×10^{-3} cm^2 V^{-1} s^{-1}.

Besides **18–23**, several other C- or N-functionalized N-heteropentacenes have been synthesized as candidates for organic semiconductors.[40,41] Among these molecules, hexaazapentacenes **24a–c** (shown in Figure 1c) reported by Zhang and coworkers [41] are promising candidates for n-channel OTFTs given that they have LUMO energy levels as low as –3.6 eV and their highly symmetric structure may facilitate easy crystallization in thin films.

5. Conclusions and Outlook

The past decade, especially the last five years, has witnessed a rapid growth of N-heteropentacenes in terms of new molecular structures, efficient synthetic methodology, better understanding of structure–property relationships, and superior performance in OTFTs. The success of N-heteropentacenes as organic semiconductors has relied and will rely on a synergy of organic synthesis, crystal engineering, and device interface engineering.

Larger N-heteroacenes, such as N-heterohexacenes and N-heteroheptacenes, are interesting π-molecules. However, for organic semiconductors, larger is not necessarily better. For example, 6,15-dihydro-6,15-diazahexacene exhibits a lower field-effect mobility than **3**.[5] Longer N-heteroacenes need to be carefully evaluated in terms of electronic structures, molecular packing, and charge transport. Unlike pentacene, N-heteropentacenes are capable of hydrogen bonds with N atoms in the solid state. The only known N-heteropentacene capable of classical H-bonds of N–H···N in the solid state is dihydrotetraazapentacene **5**, which is unfortunately not crystallized in vacuum-deposited films. Further tuning the molecular packing of N-heteropentacenes with H-bonds requires novel patterns of N atoms in the pentacene backbone. One advantage of N-heteropentacenes over pentacene is that they can be easily functionalized by direct reactions on N atoms. New N-functionalized N-heteropentacenes can be designed by changing the substituting groups and the pattern of substitution. One of the most promising applications of OTFTs is chemical and biological sensing, because OTFT-based sensors can combine the sensory electrical output with easy device fabrication. Although the N atoms of N-heteropentacenes can in principle serve as a binding site with hydrogen bonds for these sensors, fine tuning of molecular packing is necessary to allow these binding sites accessible to analyte molecules. In these directions, new opportunities lie in N-heteroacenes with unprecedented patterns and substitutions of N atoms.

Acknowledgements

This work was supported by a grant from the Research Grants Council of Hong Kong (project number: GRF402011) and the University Grants Committee of Hong Kong (project number: AoE/P-03/08). The author thanks the students and collaborators for their contributions to the research on *N*-heteropentacenes.

Received: November 5, 2013
Revised: December 3, 2013
Published online: March 2, 2014

[1] For examples of B-heteroarenes, see: a) S. Saito, K. Matsuo, S. Yamaguchi, *J. Am. Chem. Soc.* **2012**, *134*, 9130; b)L. G. Mercier, W. E. Piers, M. Parvez, *Angew. Chem. Int. Ed.* **2009**, *48*, 6108; c)A. Caruso, Jr., M. A. Siegler, J. D. Tovar, *Angew. Chem. Int. Ed.* **2010**, *49*, 4213.
[2] For examples of heteroarenes containing fused B-N, see: a) T. Hatakeyama, S. Hashimoto, S. Seki, M. Nakamura, *J. Am. Chem. Soc.* **2011**, *133*, 18614; b) A. J. Marwitz, A. N. Lamm, L. N. Zakharov, M. Vasiliu, D. A. Dixon, S.-Y. Liu, *Chem. Sci.* **2012**, *3*, 825; c) M. J. D. Bosdet, W. E. Piers, T. S. Sorensen, M. Parvez, *Angew. Chem. Int. Ed.* **2007**, *46*, 4940.
[3] O. Fischer, E. Hepp, *Chem. Ber.* **1890**, *23*, 2789.
[4] O. Hinsberg, *Ann. Chem.* **1901**, *319*, 257.
[5] Q. Miao, T.-Q. Nguyen, T. Someya, G. B. Blanchet, C. Nuckolls, *J. Am. Chem. Soc.* **2003**, *125*, 10284.
[6] a) U. H. F. Bunz, *Chem. Eur. J.* **2009**, *15*, 6780; b) G. J. Richards, J. P. Hill, T. Mori, K. Ariga, *Org. Biomol. Chem.* **2011**, *9*, 5005; c) U. H. F. Bunz, J. U. Engelhardt, B. D. Lindner, M. Schaffroth, *Angew. Chem. Int. Ed.* **2013**, *52*, 3810.
[7] Q. Miao, *Synlett*, **2012**, *23*, 326
[8] a) J. Jang, *Mater . Today* **2006**, *9*, 46; b) G. Gelinck, P. Heremans, K. Nomoto, T. Anthopoulos, *Adv. Mater.* **2010**, *22*, 3778.
[9] a) T. Someya, A. Dodabalapur, J. Huang, K. C. See, H. E. Katz, *Adv. Mater.* **2010**, *22*, 3799; b) J. T. Mabeck, G. G. Malliaras, *Anal. Bioanal. Chem.* **2006**, *384*, 343.
[10] A. R. Murphy, J. M. J. Fréchet, *Chem. Rev.* **2007**, *107*, 1066.
[11] M. L. Tang, A. D. Reichardt, P. Wei, Z. Bao, *J. Am. Chem. Soc.* **2009**, *131*, 5264.
[12] a) J.-L. Brédas, J. P. Calbert, D. A. da Silva, J. Cornil, *Proc. Natl. Acad. Sci. USA* **2002**, *99*, 5804; b) J.-L. Brédas, D. Beljonne, V. Coropceanu, J. Cornil, *Chem. Rev.* **2004**, *104*, 4931.
[13] O. Tverskoy, F. Rominger, A. Peters, H.-J. Himmel, U. H. F. Bunz, *Angew. Chem. Int. Ed.* **2011**, *50*, 3557.
[14] S. A. Jenekhe, *Macromolecules*, **1991**, *24*, 1.
[15] M. B. Casu, P. Imperia, S. Schrader, B. Falk, M. Jandke, P. Strohriegl, *Synth. Metals* **2001**, *124*, 79.
[16] Y. Ma, Y. Sun, Y. Liu, J. Gao, S. Chen, X. Sun, W. Qiu, G. Yu, G. Cui, W. Hu, D. Zhu, *J. Mater. Chem.* **2005**, *15*, 4894.
[17] Q. Tang, D. Zhang, S. Wang, N. Ke, J. Xu, J. C. Yu, Q. Miao, *Chem. Mater.* **2009**, *21*, 1400.
[18] D. Liu, Z. Li, Z. He, J. Xu, Q. Miao, *J. Mater. Chem.* **2012**, *22*, 4396.
[19] Z. He, D. Liu, R. Mao, Q. Tang, Q. Miao, *Org. Lett.* **2012**, *14*, 1050.
[20] K. Isoda, M. Nakamura, T. Tatenuma, H. Ogata, T. Sugaya, M. Tadokoro, *Chem. Lett.* **2012**, *41*, 937.

[21] J. I. Wu, C. S. Wannere, Y. Mo, P. von R. Schleyer, U. H. F. Bunz, *J. Org. Chem.* **2009**, *74*, 4343.
[22] C. A. Hunter, J. K. M. Sanders, *J. Am. Chem. Soc.* **1990**, *112*, 5525
[23] M. Winkler, K. N. Houk, *J. Am. Chem. Soc.* **2007**, *129*, 1805
[24] H.-Y. Chen, I. Chao, *ChemPhysChem*, **2006**, *7*, 2003.
[25] J. E. Anthony, *Angew. Chem. Int. Ed.* **2008**, *47*, 452.
[26] A. Maliakal, K. Raghavachari, H. E. Katz, E. Chandross, T. Siegrist, *Chem. Mater.* **2004**, *16*, 4980
[27] a) S. Miao, A. L. Appleton, N. Berger, S. Barlow, S. R. Marder, K. I. Hardcastle, U. H. F. Bunz, *Chem. Eur. J.* **2009**, *15*, 4990; b) A. L. Appleton, S. M. Brombosz, S. Barlow, J. S. Sears, J. L. Brédas, S. R. Marder, U. H. F. Bunz, *Nat. Commun.* **2010**, *1*, Article 91.
[28] a) B. D. Lindner, J. U. Engelhart, O. Tverskoy, A. L. Appleton, F. Rominger, A. Peters, H.-J. Himmel, U. H. F. Bunz, *Angew. Chem. Int. Ed.* **2011**, *50*, 8588; b) B. D. Lindner, J. U. Engelhart, O. Tverskoy, A. L. Appleton, F. Rominger, K. I. Hardcastle, M. Enders, U. H. F. Bunz, *Chem. Eur. J.* **2012**, *18*, 4627.
[29] a) Y.-Y. Liu, C.-L. Song, W.-J. Zeng, K.-G. Zhou, Z.-F. Shi, C.-B. Ma, F. Yang, H.-L. Zhang, X. Gong, *J. Am. Chem. Soc.* **2010**, *132*, 16349; b) C.-L. Song, C.-B. Ma, F. Yang, W.-J. Zeng, H.-L. Zhang, X. Gong, *Org. Lett.* **2011**, *13*, 2880.
[30] a) Z. Liang, Q. Tang, J. Xu, Q. Miao, *Adv. Mater.* **2011**, *23*, 1535; b) Z. Liang, Q. Tang, R. Mao, D. Liu, J. Xu, Q. Miao, *Adv. Mater.* **2011**, *23*, 5514.
[31] Z. He, R. Mao, D. Liu, Q. Miao, *Org. Lett.* **2012**, *14*, 4190.
[32] X.-D. Tang, Y. Liao, H. Geng, Z.-G. Shuai, *J. Mater. Chem.* **2012**, *22*, 18181.
[33] X.-K. Chen, L.-Y. Zou, J.-X. Fan, S.-F. Zhang, A.-M. Ren, *Org. Electron.* **2012**, *13*, 2832.
[34] D. Liu, X. Xu, Y. Su, Z. He, J. Xu, Q. Miao, *Angew. Chem. Int. Ed.* **2013**, *52*, 6222.
[35] E. D. Głowacki, M. Irimia-Vladu, M. Kaltenbrunner, J. Gasiorowski, M. S. White, U. Monkowius, G. Romanazzi, G. P. Suranna, P. Mastrorilli, T. Sekitani, S. Bauer, T. Someya, L. Torsi, N. S. Sariciftci, *Adv. Mater.* **2013**, *25*, 1563.
[36] S. Z. Weng, P. Shukla, M.-Y. Kuo, Y.-C. Chang, H.-S. Sheu, H.-S.; I. Chao, Y.-T. Tao, *ACS Appl. Mater. Interfaces* **2009**, *1*, 2071.
[37] M. M. Islam, S. Pola, Y.-T. Tao, *Chem. Commun.* **2011**, *47*, 6356.
[38] Q. Tang, J. Liu, H. S. Chan, Q. Miao, *Chem. Eur. J.* **2009**, *15*, 3965.
[39] T. Itoh, S. Aomori, M. Oh-e, M. Koden, Y. Arakawa, *Synth. Metals* **2012**, *162*, 1264.
[40] a) F. Wudl, P. A. Koutentis, A. Weitz, B. Ma, T. Strassner, K. N. Houk, S. I. Khan, *Pure Appl. Chem.* **1999**, *71*, 295; b) J. Fleischhauer, S. Zahn, R. Beckert, U.-W. Grummt, E. Birckner, H. Görls, *Chem. Eur. J.* **2012**, *18*, 4549; c) K. Cai, Q. Yan, D. Zhao, *Chem. Sci.* **2012**, *3*, 3175.
[41] G. Li, Y. Wu, J. Gao, C. Wang, J. Li, H. Zhang, Y. Zhao, Y. Zhao, Q. Zhang, *J. Am. Chem. Soc.* **2012**, *134*, 20298.